

# Electronic structure and optical properties of B- or N-doped graphene adsorbed methanol molecule: first-principles calculations

WEN WANG<sup>a</sup>, XIUWEN ZHAO<sup>b</sup>, JUNFENG REN<sup>b,\*</sup>

<sup>a</sup>CNGC Institute 53, Jinan, 250031, China

<sup>b</sup>School of Physics and Electronics, Shandong Normal University, Jinan, 250014, China

Comprehensive calculations of the various geometrical structures, band structures and the optical properties for B, N-doped graphene adsorbed methanol molecule are performed by means of first-principles calculations. It is found that the band gap appears and the optical parameters change as well. The maximum values of the dielectric constants, the refractive index and the reflectivity increase after the doping and the adsorption. The effects of N doping on the optical properties are bigger than that of B doping because of the more  $\pi$  electrons. Methanol molecule adsorption has obvious impact on the optical properties of N-doped graphene, which shows that the interaction between N-doped graphene and methanol is relatively strong, so N-doped graphene can be used to adsorb and detect methanol molecule.

(Received March 19, 2020; accepted February 15, 2021)

**Keywords:** Electronic structure, Optical properties, Doped-graphene, Molecular adsorption

## 1. Introduction

It is well known that graphene was stripped from graphite in the year of 2004. Graphene is a magical two-dimensional material with a variety of remarkable functions based on its single layer honeycomb lattice which is formed by  $sp^2$  hybrid of carbon atoms. [1-3]. Graphene has excellent conductivity, large specific surface area, outstanding thermal conductivity and perfect quantum tunneling effect, etc. Optical properties of graphene have been extensively studied in both theory and experiments and the interests in the study of graphene in photonic and optoelectronics are also rising which is shown by its various applications, such as solar cells, lighting-emitting and touch screen, etc [4-11]. Pristine graphene has zero band gap, its electrons and holes obey the two-dimensional Dirac equation and energy band structure near the Fermi level shows linear dispersion relation [12-14]. Zero band gap structure limits the development of pristine graphene in the field of nanoelectronics and optoelectronic devices. In recent years, the electronic and optical structures of graphene and its derivatives have been studied and significant modifications of graphene were noted [15-19].

There are various methods to optimize the band structure and modify the optical properties of graphene which are related to band structures directly. One method is doping foreign atoms such as N and B, whose atomic radii are close to that of carbon atoms, which will not induce big lattice distortion. In addition, foreign atoms

usually have different electronic configuration comparing with C atom, so charge transfer will occur after the doping, then the electronic and optical properties of graphene will be significantly optimized [20-22]. Another method is adsorbing atoms or molecules, such as CO, NO, NO<sub>2</sub> and thiophene molecule, etc. As graphene has only one atomic layer thickness and is easily exposed to the outside world, the atoms and molecules adsorbed on the surface of graphene can change the structure of the graphene by perturbing the  $\pi$ -electron network [23-25]. For example, Wang et al. studied the adsorption of CO molecules on doped graphene, which suggested that doped graphene is more sensitive than pristine graphene to the adsorption of CO [26]. Besides, the topological disorders like ripples and Stone-Wales defects are also important in optimizing the properties of graphene as well [27-28].

Gas sensors based on graphene adsorbed different molecules especially pollutants have attracted many researcher's interests. Methanol is one of the basic organic raw materials, its toxicity has great impact on body's nervous system and blood systems, and it needs to be detected. The adsorption of methanol molecule on pristine graphene have been studied and it shows that no obvious effect occurs on the electronic structure and the optical properties. However, the sensitivity of graphene can be enhanced by doping techniques, so as a candidate for gases sensor, graphene plays an important role in gas detection [26]. It is worth mentioning that the modeling works of graphene and graphene-like systems in relation to B and N have been studied widely [29-32]. In order to improve the

sensitivity for methanol molecule in graphene, we also choose B and N atoms as dopants to study the changes of the electronic structures and the optical properties, which corresponds to the widely used p-type and n-type doping methods, respectively. The structure of the article is as follows: the theoretical calculation methods are shown in Section 2, the results analysis are given in Section 3, and a conclusion is listed in Section 4.

## 2. Methods

All our theoretical calculations are done through VASP (Vienna ab-initio Simulation Package) [33]. A  $4 \times 4 \times 1$  supercell (32 atoms) of pristine graphene is chosen as the sheet [18-19]. One carbon atom in the graphene sheet is substituted by B or N atom, which are called BG and NG systems. A methanol molecule is adsorbed on the surface of BG and NG, which are named as BGM and NGM systems, respectively. The modified electronic and optical properties of NG, BG, NGM and BGM systems have been explored with respect to the two different kinds of impurities. PAW pseudopotential is used to describe the interaction between ions and electrons [34]. For the energy exchange correlation energy function, the generalized gradient approximation (GGA) in the form of Perdew-Burke-Ernzerhof (PBE) are used [35]. The cut-off energy is 400 eV in the process of structural optimizations and calculations. A  $7 \times 7 \times 1$  Monkhorst-Pack grid is chosen when calculate integral in Brillouin zone. Energy convergence is set to less than  $10^{-4}$  eV and the convergence accuracy of the nuclear motion is set to less than 0.2 eV/Å. The thickness of the vacuum layer is set to 15 Å in order to avoid the interlayer interference. The van der Waals interactions DFT-D3 are included in the calculations.

The optical properties are general evaluated by the dielectric function, which is the sum of the real and the imaginary parts,  $\varepsilon(\omega) = \varepsilon_1(\omega) + i\varepsilon_2(\omega)$ . The imaginary part is calculated by the summations of the empty band states using the following equation [36],

$$\varepsilon_2(\omega) = \frac{4\pi^2 e^2}{\Omega} \lim_{q \rightarrow 0} \frac{1}{q^2} \sum_{c,v,k} 2w_k \delta(\varepsilon_{ck} - \varepsilon_{vk} - \omega) \times \langle u_{ck} + e_{\alpha q} | u_{vk} \rangle \langle u_{ck} + e_{\beta q} | u_{vk} \rangle^* \quad (1)$$

where  $\omega$  represents the frequency of electromagnetic (EM) radiation in energy unit.  $\Omega$  represents the volume,  $v$  and  $c$  correspond to the valence and the conduction bands respectively,  $\alpha$  and  $\beta$  indicate the Cartesian components,  $e_\alpha$  and  $e_\beta$  are the vacuum dielectric constants,  $\varepsilon_{ck}$  and  $\varepsilon_{vk}$  refer to the energy of the conduction and the valence band respectively,  $u_{ck}$  is the cell periodic part of the orbitals at the k-point. The real part of the dielectric tensor is calculated by the Kramers-Kronig relation,

$$\varepsilon_1(\omega) = 1 + \frac{2}{\pi} P \int_0^\infty \frac{\varepsilon_2^\alpha(w') w'}{w'^2 - w^2 + i\eta} dw', \quad (2)$$

where P denotes the principle value. According to the values of the real and the imaginary part of dielectric tensor, the optical properties such as the absorption coefficient  $\alpha(\omega)$ , the refractive index  $n(\omega)$ , the reflectivity  $R(\omega)$  and the electron energy loss spectroscopy  $L(\omega)$  can be given by [37-38],

$$\alpha(\omega) = \frac{\sqrt{2}\omega}{c} \left\{ [\varepsilon_1^2(\omega) + \varepsilon_2^2(\omega)]^{\frac{1}{2}} - \varepsilon_1(\omega) \right\}^{\frac{1}{2}}, \quad (3)$$

$$n(\omega) = \frac{1}{\sqrt{2}} \left\{ [\varepsilon_1^2(\omega) + \varepsilon_2^2(\omega)]^{\frac{1}{2}} + \varepsilon_1(\omega) \right\}^{\frac{1}{2}}, \quad (4)$$

$$R(\omega) = \frac{\left| \frac{\sqrt{\varepsilon_1(\omega) + i\varepsilon_2(\omega)} - 1}{\sqrt{\varepsilon_1(\omega) + i\varepsilon_2(\omega)} + 1} \right|^2}{}, \quad (5)$$

$$L(\omega) = \frac{\varepsilon_2(\omega)}{\varepsilon_1^2(\omega) + \varepsilon_2^2(\omega)}. \quad (6)$$

## 3. Results and discussion

There are several adsorption configurations both for BGM and NGM systems, i.e. top, hollow and bridge site adsorptions, which correspond to the top of B and N dopants, the center of the hexatomic ring including the dopants, the center of the bond between carbon atom and the dopants. For each configuration, the oxygen atom or the hydrogen atom connected to it in the methanol molecule is placed on the corresponding sites. After fully relaxed, it is found that the energy will be the minimum when H atom is adsorbed on the top of B or N atom, and the fully relaxed structures are shown in Fig.1. For these two cases, the distances between the H atom and the B or N atom are 2.37 Å and 2.54 Å, which is defined as the adsorption distance, respectively. The bond lengths of C<sub>1</sub>-C<sub>2</sub> in the graphene sheet and C<sub>3</sub>-O in the methanol molecule keep almost unchanged after the adsorptions. The adsorption energy is also calculated for the two systems. The adsorption energy is used to reflect the strength of the adsorption, which is generally negative, i.e., the greater absolute value of the adsorption energy means the more stable system. The adsorption energy  $E_{ad}$  is calculated as  $E_{ad} = E_{tot} - E_g - E_m$ , where  $E_{tot}$ ,  $E_g$  and  $E_m$  are the total energy of the whole system, the energy of B- or N-doped graphene and the energy of methanol molecule, respectively. The adsorption energies are -0.05 eV and -0.17 eV for BGM and NGM systems, respectively, which means that the NGM system is more stable than BGM system.

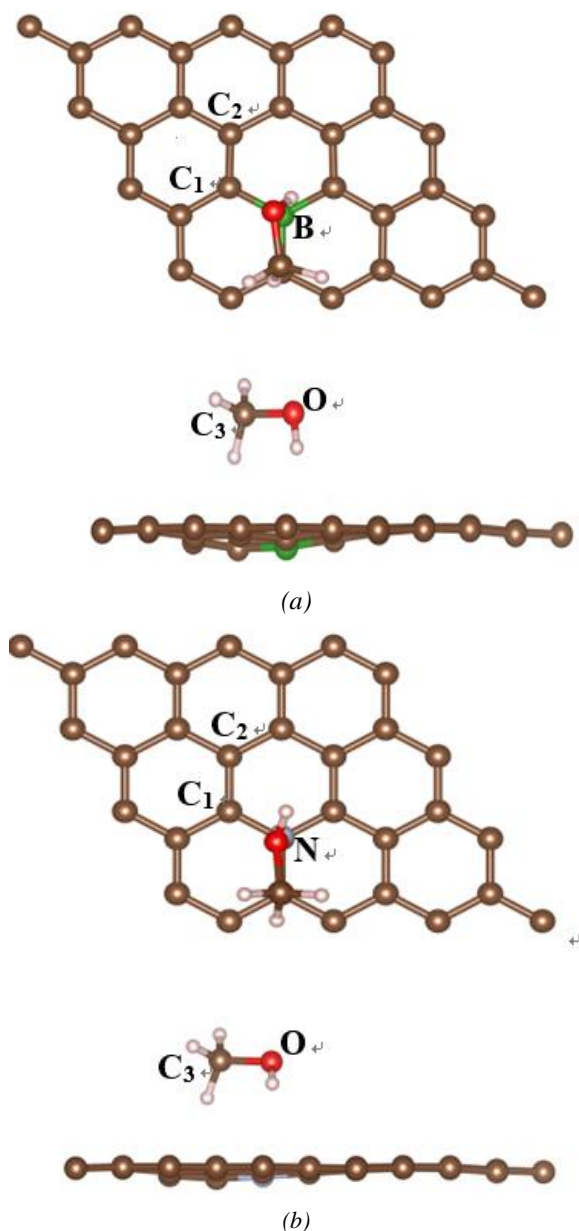


Fig.1. Top and side views of the relaxed structures. (a) BGM system (b) NGM system. Red, white, brown, green and gray spheres represent O, H, C, B and N atoms, respectively.

To further study the effects of methanol molecule adsorption on the electronic properties of graphene, the band structures are calculated. For comparison, we also calculate the band structure of pristine graphene, BG, NG, BGM and NGM systems. It can be found that the band gap of pristine graphene is zero, which is consistent with previous works [12-14]. And the adsorption distance is bigger than 3 Å, which means that the effect of methanol molecule adsorption is weak. The band structure of BG, NG, BGM and NGM systems are shown in Fig. 2. It is found from Fig. 2(a) that the NG system has a band gap of about 0.18 eV, and the Fermi level elevated to the conduction band, these results are originated from the fact that the N atom has one more electron than that of

the C atom, so N atom in graphene acts as an n-dopant. For BG system, the results are shown in Fig. 2(c), the band gap is similar to that of N-doped graphene, while the Fermi level descended to the valence band, so B in graphene acts as a p-dopant, these results are consistent with previous reports [39]. By doping B or N atoms, the band structure of graphene changes, but the effect of methanol molecule adsorption is not significant, the band structures of NGM and BGM systems are similar to NG and BG systems, respectively, which means that the molecule adsorption has little impact on band gap of NG and BG systems.

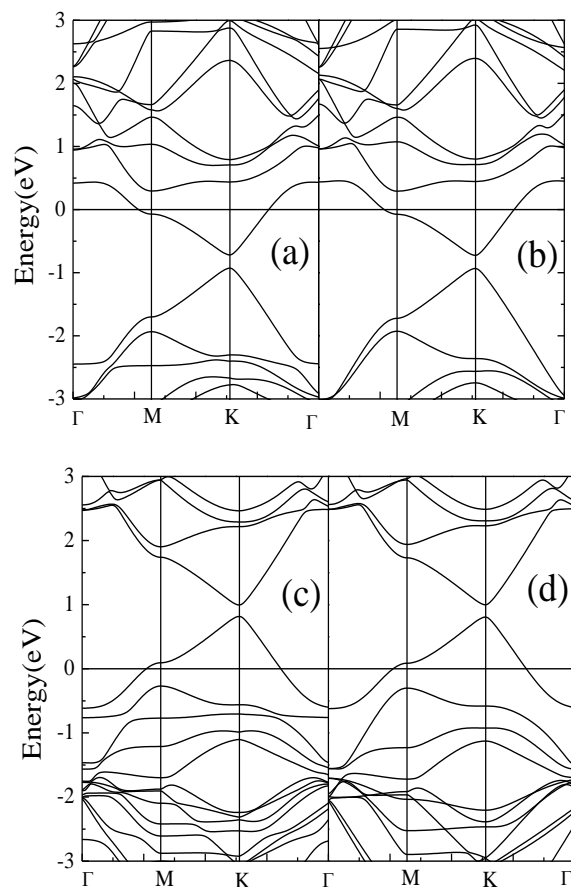


Fig. 2. Band structures of different systems. (a) NG, (b) NGM, (c) BG, (d) BGM

The projected density of states (PDOS) for NG, NGM, BG, BGM systems have also given, which are shown in Fig. 3. Fig. 3 shows that the PDOS are in line with the band structures in Fig. 2. Fermi level moves to the conduction band for NG system and the Fermi level moves to the valence band for BG system. After introducing the dopant and methanol molecule to the graphene system, the PDOS changed. From the Fig. 3(a) and (b), it can be seen that the density of states are mainly composed of the p orbit of carbon atoms. While for BGM and NGM systems, there are hybridization of the p orbital between oxygen and carbon atoms, and the hybridization is more prominent for NGM system, which means that N-doped graphene is more suitable to adsorb methanol molecule. In addition,

the charge transfers ( $\Delta Q$ ) from methanol molecule to graphene are also given of BGM and NGM systems. It is clear that the NGM system has a bigger value of 2.63e than 0.72e for BGM system, which means that the methanol molecule and graphene system has the most distinct interaction for NGM systems.

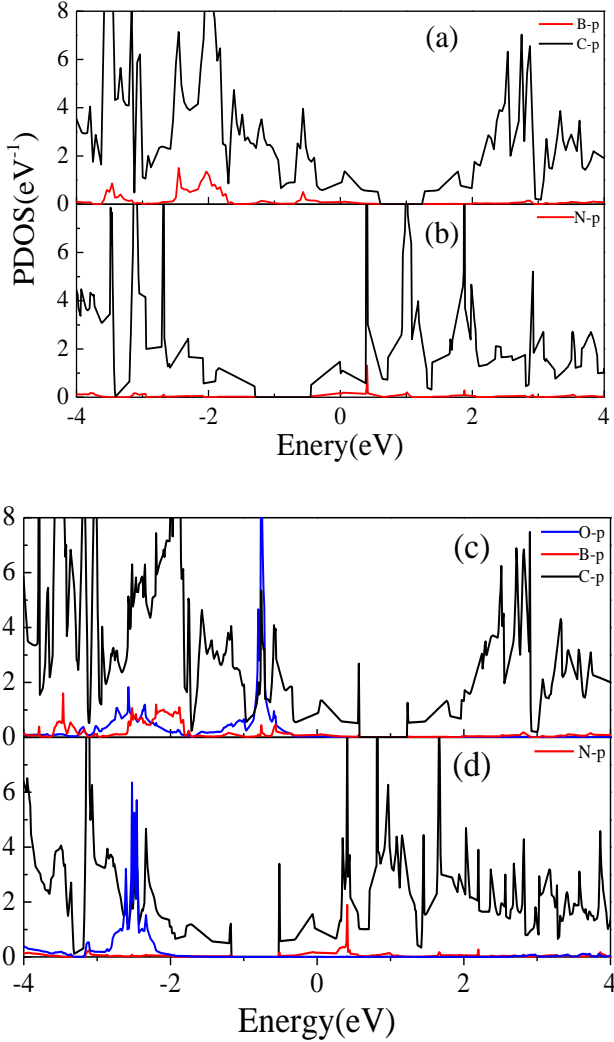


Fig. 3. Projected density of states (PDOS) for different doping systems. (a) BG, (b) NG, (c) BGM, (d) NGM

It is evident from the previous calculations that the electronic structures of graphene change, so the optical properties will also be modified. Fig. 4 shows the dielectric function of the pristine graphene. As we all know, the dielectric tensor in the hexamer lattice has two independent components,  $\epsilon_{xx}(\omega)$  along a-axis and  $\epsilon_{zz}(\omega)$  along c-axis. From our calculations, we found that the doping and adsorption have little impact on  $\epsilon_{zz}(\omega)$ , so the optical constants along a-axis  $\epsilon_{xx}(\omega)$  are mainly considered. From Fig. 4(a), it is found that the real part  $\epsilon_1$  along a-axis of the dielectric function of pristine graphene has values less than zero when the energy is about 4 eV, the maximum of  $\epsilon_1$  around zero energy is 6.41. From table 1, it is found that the maximum for BG and BGM systems

are similar to that of the pristine graphene. However, for NG and NGM systems, the maximum of  $\epsilon_1$  increases drastically, which is 19.24 and 14.70, respectively. Fig. 4(d) represents the imaginary part  $\epsilon_2$  of the dielectric function. It is obvious that  $\epsilon_2$  of pristine graphene have significant peaks at small energy region (0-5 eV) and high energy region (near the 14 eV), these peaks are attributed to  $\pi \rightarrow \pi^*$  and  $\sigma \rightarrow \sigma^*$  interband transitions, respectively [41]. The maximum of  $\epsilon_2$  for pristine graphene is 4.10, and it has little change in BG system compared with pure graphene, however, it increases significantly in NG system, which are shown in Table 1. In addition, after adsorbed the methanol molecule, the maximums for both  $\epsilon_1$  and  $\epsilon_2$  decrease. It can be concluded that the dielectric function of NGM system is significantly different from pristine graphene and BGM system, the interaction between methanol molecule and N-doped graphene has certain enhancement.

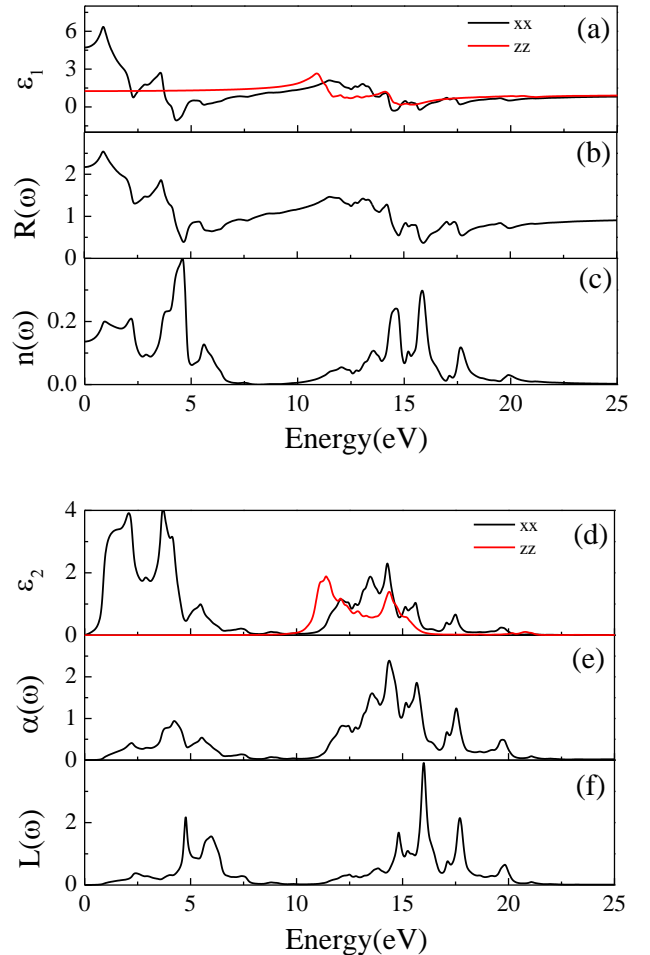


Fig. 4. Optical properties of pristine graphene. (a) real part of dielectric function, (b) reflectivity, (c) refractive index, (d) imaginary part of dielectric function, (e) adsorption coefficient, (f) energy-loss function

The refractive index  $n(\omega)$  and reflectivity  $R(\omega)$  of pristine graphene are shown in Fig. 4(b) and (c), respectively. It is found that the maximum of the refractive index  $n(\omega)$  for pristine graphene is 2.63, this value is

consistent with previous theoretical calculations but is smaller than experimental value [6, 18]. It is obvious that for the BG and BGM systems, no noticeable change of the  $n(\omega)$  maximum value has been observed compared with that of pristine graphene. For NG and NGM systems, the maximum value increases significantly, they are about 4.57 and 4.00, and it can be seen that the methanol molecule adsorption reduced the maximum value of  $n(\omega)$  for both BG and NG systems as well. It is noticeable from Fig. 4(c) that the prominent peaks of the reflectivity can be observed around at 4.5 eV and 15.0 eV, and it is very small or almost zero in the region of 7.0 eV-10.0 eV. The value of  $\varepsilon_2(\omega)$  is very small in the region of 7.0 eV-10.0 eV as shown in Fig. 4(d), therefore a very small value of reflectivity is expected in this region accordingly. Compared with pristine graphene, the maximum of  $R(\omega)$  for BG and BGM systems decreases, however, it increases for NG and NGM systems, all these results are shown in Table 1. The maximum value of  $R(\omega)$  for NG and NGM systems are lying within the visible to infrared region. Due to the addition of extra  $\pi$  electrons in the NGM system by N doping, an obvious peak occurs at about 0.5 eV, which is different from pristine graphene and BGM system [18].

Table 1. Maximums of the optical parameters for different systems

Systems	graphene	BG	BGM	NG	NGM
$\varepsilon_1$	6.41	6.65	6.50	19.24	14.70
$\varepsilon_2$	4.10	3.98	3.76	118.77	15.98
$n(\omega)$	2.63	2.59	2.50	4.57	4.00
$R(\omega)$	0.39	0.21	0.21	0.48	0.46
$\alpha(\omega)/10^5$	2.32	2.00	1.70	1.56	1.40

The absorption coefficient  $\alpha(\omega)$  is directly connected to the imaginary part of the dielectric function, which is depicted in Fig. 5. It can be seen that the adsorption index is zero when energy is near the zero and there are two peaks at about 4.2 eV and 14.5 eV respectively, the results are agreement with the previous works [6, 18]. It can be observed that the highest peaks decrease significantly for BG, BGM, NG and NGM systems. The absorbance is almost zero within the energy interval 7.0 eV-9.0 eV, which is consistent with the reflectivity. It is clear that the pristine graphene as well as BG, NG, BGM and NGM systems are highly transparent around the energy range 7.0 eV-9.0 eV. In other words, compare reflectivity and absorbance, it can be found that if one system can strongly adsorb the light in a spectral range, they can reflect the light in the same spectral range effectively. In addition, the peak position of  $\alpha(\omega)$  for N-doped systems move to high energy range compared with B-doped systems and pristine graphene, and after adsorbed methanol molecule, the peak position shift a lot.

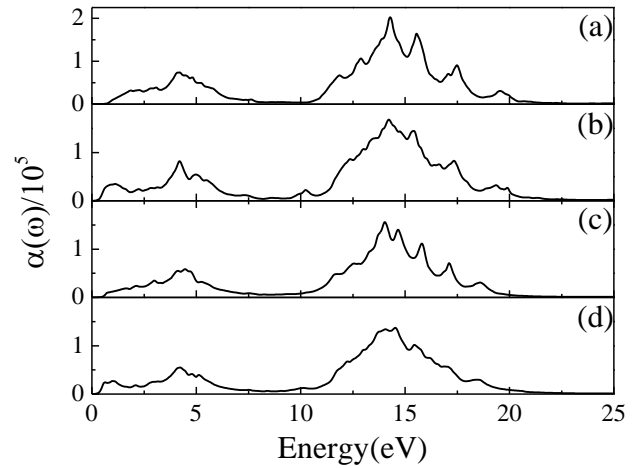


Fig. 5. Adsorption index of different systems. (a) BG, (b) NG, (c) BGM, (d) NGM

The electron energy loss spectrums  $L(\omega)$  have been depicted for different systems, which are shown in Fig. 6. For the  $L(\omega)$  of pristine graphene, two prominent peaks have been observed at 4.8 eV and 15.8 eV. Experimental and theoretical in-plane plasmon excitation peaks have been observed at 4.7 eV and 14.6 eV due to  $\pi$  and  $(\pi + \sigma)$  plasmons, respectively [41]. For BG, NG, NGM and BGM systems, the peaks decrease obviously compared with those of pristine graphene, and the peaks of NGM system drop more than BGM system. In addition, compared with BG, BGM and pristine graphene, a new peak around 1.4 eV has been observed in NG and NGM systems. And in the energy range of 14 to 17 eV, the peaks of NGM system is different from other systems.

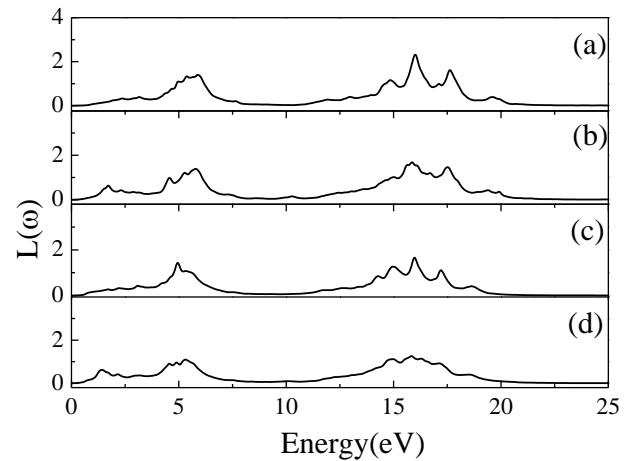


Fig. 6. Electron energy loss spectrums of different systems. (a) BG, (b) NG, (c) BGM, (d) NGM, respectively

#### 4. Conclusions

In summary, we studied the structural, electronic and optical properties of B- and N-doped graphene adsorbed methanol molecule through first principles calculations. After doping and adsorption, it can be observed that

band gap appears and the dielectric function, adsorption coefficient, refractive index, reflectivity and electron energy loss spectroscopy change significantly compared with pristine graphene. For NG and NGM systems, the maximum of the real and imaginary parts of the dielectric constant, refractive index and the reflectivity increase significantly than those of the BG, BGM systems and pristine graphene. The peaks of adsorption coefficient for NG and NGM systems shift slightly compared with BG, BGM systems and pristine graphene. The transparency is high around the energy range of 7.0 eV-9.0 eV for all systems. A sharp electron energy loss spectroscopy peak arises for NG and NGM systems around 1.4 eV, and the peaks of NGM system is different from other systems in the energy range of 14 to 17eV. All these calculations show that NGM system has more significant impact on the optical properties, which can be used to adsorb and detect methanol molecule. Optical properties such as adsorption index and electron energy loss spectrums of graphene are affected by the molecule adsorption, so graphene could be used as sensors to detect molecules based on the changes of the optical properties of the system. All these results can help to understand the properties of optoelectronic materials involving graphene.

### Acknowledgments

The authors would like to acknowledge the financial support from the National Natural Science Foundation of China (Grant No. 11674197) and the Natural Science Foundation of Shandong Province (Grant No. ZR2018MA042). Thanks to the supporting of Taishan Scholar Project of Shandong Province.

### References

- [1] K. S. Novoselov, A. K. Geim, S. V. Morozov, D. Jiang, Y. Zhang, S. V. Dubonos, I. V. Grigorieva, A. A. Firsov, *Science* **306**, 666 (2004).
- [2] Y. Zhang, J. Small, P. Kim, *Phys. Rev. Lett.* **94**, 176803 (2005).
- [3] S. Stankovich, D. A. Dikin, G. H. B. Dommett, K. M. Kohlhaas, E. J. Zimney, E. A. Stach, R. D. Piner, S. T. Nguyen, R. S. Ruoff, *Nature* **442**, 282 (2006).
- [4] Y. Wang, Z. S. Qu, J. Liu, Y. H. Tsang, *J. Lightwave Technol.* **30**, 3259 (2012).
- [5] R. Kurapati, K. Kostarelos, M. Prato, A. Bianco, *Adv. Mater.* **28**, 6052 (2016).
- [6] H. Zhu, J. Liu, S. Jiang, S. Xu, L. Su, D. Jiang, X. B. Qian, J. Xu, *Opt. Laser Technol.* **75**, 83 (2015).
- [7] X. Chen, R. Meng, J. Jiang, Q. Liang, Q. Yang, C. Tan, X. Sun, S. Zhang, T. Ren, *Phys. Chem. Chem. Phys.* **18**, 16302 (2016).
- [8] H. Rezaia, M. Yarmohammadi, *Opt. Mater.* **57**, 8 (2016).
- [9] Y. Y. Ren, G. Brown, R. Mary, G. Demetriou, D. Popa, F. Torrisi, A. C. Ferrari, F. Chen, A. K. Kar, *IEEE J. Sel. Top. Quant.* **21**, 1602106 (2015).
- [10] F. J. Nelsona, V. K. Kamineni, T. Zhang, E. S. Comfort, J. U. Lee, *Appl. Phys. Lett.* **97**, 253110 (2010).
- [11] J. W. Weber, V. E. Calado, M. C. M. van de Sanden, *Appl. Phys. Lett.* **97**, 091904 (2010).
- [12] A. H. Castro Neto, F. Guinea, N. M. R. Peres, K. S. Novoselov, A. K. Geim, *Rev. Mod. Phys.* **8**, 109 (2009).
- [13] D. S. L. Abergel, V. Apalkov, J. Berashevich, K. Ziegler, T. Chakraborty, *Adv. Phys.* **59**, 261 (2010).
- [14] C. N. R. Rao, A. K. Sood, K. S. Subrahmanyam, A. Govindaraj, *Angew. Chem. Int. Edit.* **48**, 7752 (2009).
- [15] D. Jana, C. L. Sun, L. C. Chen, K. H. Chen, *Prog. Mater. Sci.* **58**, 565 (2013).
- [16] X. W. Zhao, B. Qiu, W. W. Yue, G. C. Hu, J. F. Ren, X. B. Yuan, *Eur. Phys. J.* **92**, 44 (2019).
- [17] D. Jana, L. C. Chen, C. W. Chen, S. Chattopadhyay, *Carbon* **45**, 1482 (2007).
- [18] P. Nath, S. Chowdhury, D. Sanyal, D. Jana, *Carbon* **73**, 275 (2014).
- [19] B. Qiu, X. W. Zhao, G. C. Hu, W. W. Yue, X. B. Yuan, J. F. Ren, *Physica E* **116**, 113729 (2020).
- [20] X. K. Kong, C. L. Chen, Q. W. Chen, *Chem. Soc. Rev.* **43**, 2841 (2014).
- [21] B. Qiu, X. W. Zhao, Y. Li, R. D. Liang, G. C. Hu, X. B. Yuan, J. F. Ren, *Physics Letters A* **384**, 126663 (2020).
- [22] Z. Xie, X. Zuo, G. P. Zhang, Z. L. Li, C. K. Wang, *Chem. Phys. Lett.* **657**, 18 (2016).
- [23] X. B. Yuan, M. S. Yang, Y. L. Tian, L. L. Cai, J. F. Ren, *Synthetic. Meta.* **226**, 46 (2017).
- [24] A. S. Rad, *Appl. Surf. Sci.* **357**, 1217 (2015).
- [25] Y. L. Tian, J. F. Ren, W. W. Yue, M. N. Chen, G. C. Hu, X. B. Yuan, *Chem. Phys. Lett.* **685**, 344 (2017).
- [26] W. Wang, Y. Zhang, C. Shen, Y. Chai, *AIP. Adv.* **6**, 025317 (2016).
- [27] J. Ma, D. Alfè, A. Michaelides, E. Wang, *Phys. Rev. B* **80**, 033407 (2009).
- [28] S. Chowdhury, S. Baidya, D. Nafday, S. Halder, *Physica E* **61**, 191 (2014).
- [29] E. Broitman, G. K. Gueorguiev, A. Furlan, N. T. Son, A. J. Gellman, S. Stafström, L. Hultman, *Thin Solid Films* **517**, 1106 (2008).
- [30] N. Hellgren, T. Berlind, G. K. Gueorguiev, M. P. Johansson, S. Stafström, L. Hultman, *Mat. Sci. Eng. B.* **113**, 242 (2004).
- [31] G. K. Gueorguiev, E. Broitman, A. Furlan, S. Stafstr, L. Hultman, *Chem. Phys. Lett.* **482**, 110 (2009).
- [32] F. Schedin, A. K. Geim, S. V. Morozov, E. W. Hill, P. Blake, M. I. Katsnelson, K. S. Novoselov, *Nat. Mater.* **6**, 652 (2007).

- [33] G. Kresse, J. Furthmüller, *Comp. Mater. Sci.* **6**, 15 (1996).
- [34] G. Kresse D. Joubert, *Phys. Rev. B* **59**, 1758 (1999).
- [35] J. P. Perdew, K. Burke, M. Ernzerhof, *Phys. Rev. Lett.* **77**, 3865 (1996).
- [36] M. Gajdoš, K. Hummer, G. Kresse, J. Furthmüller, *Phys. Rev. B* **73**, (2006) 045112.
- [37] S. Saha, T. P. Sinha, A. Mookerjee, *Phys. Rev. B* **62**, 8828 (2000).
- [38] B. Luo, X. Wang, E. Tian, G. Li, L. Li, *J. Mater. Chem. C* **3**, 8625 (2015).
- [39] Y. C. Zhou, H. L. Zhang, W. Q. Deng, *Nanotechnology* **24**, 225705 (2013).
- [40] A. G. Marinopoulos, L. Reining, A. Rubio, V. Olevano, *Phys. Rev. B* **69**, 245419 (2004).
- [41] T. Eberlein, U. Bangert, R. R. Nair, R. Jones, M. Gass, A. L. Bleloch, K. S. Novoselov, A. Geim, P. R. Briddon, *Phys. Rev. B* **77**, 233406 (2008).

---

\* Corresponding author: renjf@sdu.edu.cn